Geophys. J. Int. (1990) **103,** 657–673

Accounting for crustal magnetization in models of the core magnetic field

Andrew Jackson

Department of Earth and Planetary Sciences, Harvard University, Cambridge, Massachusetts 02138, *USA*

Accepted 1990 July 3. Received 1990 June 8; in original form 1990 March 23

SUMMARY

Remanent and induced magnetization occurs in crustal materials when they are below their Curie temperature, and we consider the problem of determining the magnetic field originating in the earth's core in the presence of such magnetization. Simple physical models of induced magnetization which have been proposed and which lead to deterministic effects account for only a small proportion of the high-degree internal field found using *Magsat* data, and thus a stochastic description appears more useful. We investigate the effect of remanent magnetization in the crust on satellite measurements of the core magnetic field by posing the question: if the crustal magnetization is correlated only on the shortest possible length-scale, and different components are uncorrelated everywhere, what is the correlation length-scale at a radius above the earth's surface? Using an idea due to Parker (1988), we model the crust as a zero-mean, stationary, Gaussian random process. We show that the matrix of second-order statistics is proportional to the Gram matrix, which depends only on the inner-products of the appropriate Green's functions, and that at a typical satellite altitude of 400 km the data are correlated out to an angular separation of approximately 15°. Accurate and efficient means of calculating the matrix elements are given. This theory leads to a more conservative form for the correlation in the data than that previously given by Langel, Estes & Sabaka (1989), whilst not being incommensurate with the imprecisely known high-degree power spectrum. Previous studies examining the core field have treated satellite data as independent, and have given different orthogonal components equal weight. Both these assumptions are incorrect, and we show that the variance of measurements of the radial component of magnetic field due to the crust is expected to be approximately twice that in horizontal components. However, the size of the crustal effect is small compared to the random noise in the data, and may not lead to radically different results from those already published.

Key words: core magnetic field, crustal magnetization, stochastic representation.

1 INTRODUCTION

Determination of the magnetic field originating in the earth's core from measurements taken at or above the earth's surface is currently of great interest. Knowledge of its morphology and time-evolution is essential for testing such ideas as whether magnetic diffusion is absent at the top of the core on the decade time-scale (the frozen-flux hypothesis of Roberts & Scott 1965) and for determining fluid flow immediately below the core–mantle boundary (CMB); it may also ultimately give insights into the mechanism responsible for the regeneration of the field over time-scales of millions of years.

It is likely that improvements in our knowledge of the core field will come from both new data from satellite missions and observatories, and from theoretical developments. For example, the effect that the conductivity of the mantle will have on magnetic signals on their passage from the core to the earth's surface has been considered (Benton & Whaler 1983; Backus 1983), but lack of knowledge of the mantle conductivity profile has prevented the use of these theories in construction of core fields. However, the effect of both remanent and induced magnetization attributable to minerals within the lithosphere which are above their Curie temperatures has been largely ignored.

Considerable attention has been given to the methods of

constructing plausible maps of the radial field B_r at the CMB (e.g. Whaler & Gubbins 1981; Shure, Parker & Backus 1982; Parker & Shure 1982; Gubbins 1983; Gubbins & Bloxham 1985; Shure, Parker & Langel 1985; Backus 1988a,b, 1989; Parker, Constable & Stark 1989). Whilst the methods of harmonic splines (HS) (Shure *et al.* 1982) and stochastic inversion (SI) (Gubbins 1983) can produce almost identical results [compare for example the models of Shure *et al.* (1985) and Gubbins & Bloxham (1985)], they choose just one smooth model from the large number which fit the data acceptably and the questions of model uniqueness are still unclear; the method of confidence set inference (CSI) may answer these questions (see Backus 1989). The purpose of this paper is not to address the question of model construction, but rather to concentrate on the statistical assumptions about the data necessary for a solution to be constructed. The results of this paper are applicable to any method of model construction, either HS, SI or CSI.

Measurements of the internal magnetic field are contaminated by external fields and observational errors. From a theoretical point of view, external fields can be separated from internal fields uniquely if an infinite amount of perfect data is available, using Gauss's classical method. Unfortunately, the internal field is derived from both the core field and from crustal magnetization, and despite views to the contrary, the two are fundamentally inseparable on the basis of the data alone. Additional, plausible assumptions about the nature of the fields can alleviate the problem, and indeed, by assuming that the crustal field has a 'white' power spectrum it is possible to treat it as random noise superposed on the longer wavelength field originating in the core. This viewpoint leads to the treatment of individual observations made by ships, surveys and observatories at the earth's surface $r = a$ (i.e. immediately above the source region) as being independent. This crucial point, that the observations are made for all practical purposes at the noise source, does not hold for satellite measurements and a more careful treatment is necessary.

It has been recognized for many years that the power spectrum of the field represents a composite of fields due to the crust and core. High-degree signals are acknowledged to be attributable to the crust, although the sources are not well understood. It is possible that the sources are well described by both deterministic and stochastic models, a division which has proved useful in statistical investigations in other fields (see e.g. Goff & Jordan 1988). It has been suggested that induced magnetization is responsible for the major part of the crustal signal (e.g. Hahn *et al.* 1984), originating from a simple deterministic model of susceptibility in the crust. One of the major emphases of this paper is to investigate whether such simple deterministic effects are discernable in the data, and whether a mixed deterministic–stochastic or purely stochastic description of the crust is more appropriate.

Satellite measurements of the magnetic field $\mathbf{B}$ are typically taken at several hundreds of kilometres above the earth's surface (e.g. between roughly 350 and 550 km in the case of the satellite *Magsat*), and these altitudes lead to some averaging of crustal fields through the action of the appropriate Green's function. Therefore, to prevent the mapping of these correlated signals into a false core field, a method is required to explicitly account for these correlations; this is performed by prescribing the crustal covariance matrix $\mathbf{C}_c$ which is part of the full data covariance matrix $\mathbf{C}_e$. We adopt a very simple statistical model, due originally to Parker (1988), to treat the averaging. We take each component of magnetization to be a stationary, zero-mean random Gaussian process, which enables the calculation of the elements of the crustal magnetization covariance $\mathbf{C}_c$ everywhere above the earth's surface. Apart from the work of Langel *et al.* (1989), every other treatment of satellite data has assumed each datum to be an independent observable, which leads to a diagonal form for the matrix $\mathbf{C}_e$. For an example of correlation in the temporal domain, and the resulting data covariance matrix $\mathbf{C}_e$ applicable to observatories and repeat stations, see Bloxham & Jackson (1989).

The content of the paper is as follows. Section 2 reviews the gross statistics of the crustal field inferred from satellite data. Section 3 explores the possibility that some of the high-degree signal may be due to deterministic effects, as has been suggested by other authors. In Section 4 we introduce a stochastic representation of the crust and describe the theory necessary for calculating the correlation functions from which relevant elements of $\mathbf{C}_c$ are calculated for typical satellite measurements. Section 5 discusses the implications of this theory and compares it with previously published methods of calculating covariance.

2 STATISTICS OF THE MAGNETIC FIELD

The satellite *Magsat* has enabled the production of high-resolution models of the earth's magnetic field which have bearing on both the field due to the core and the crustal field (e.g. Arkani-Hamed & Strangway 1986; Cain *et al.* 1989). The method usually adopted to represent the field in a source-free region is in terms of a spherical harmonic series, where the field $\mathbf{B} = -\nabla V$ and

$$V = a \sum_{l=1}^{\infty} \sum_{m=0}^{l} \left(\frac{a}{r}\right)^{l+1} (g_l^m \cos m\phi + h_l^m \sin m\phi) P_l^m(\cos\theta). \tag{1}$$

Here a is the earth's radius (taken as $a = 6371.2$ km), the $\{g_l^m; h_l^m\}$ are the geomagnetic or Gauss coefficients and the $P_l^m(\cos\theta)$ are Schmidt quasi-normalized Legendre functions conventional in geomagnetism which satisfy

$$\int (P_l^m)^2 \sin^2 m\phi \, d\Omega = \int (P_l^m)^2 \cos^2 m\phi \, d\Omega = \int (P_l^0)^2 \, d\Omega = \frac{4\pi}{2l+1}, \tag{2}$$

where $d\Omega$ signifies integration over solid angle. More general representations are available in regions where currents cannot be neglected (e.g. Backus 1986). When the representation (1) is adopted, then the power in the magnetic field $|\mathbf{B}|^2$ at radius a can be written (Mauersberger 1956; Lowes 1966)

$$|\mathbf{B}|^2 = \sum_{l=1}^{\infty} R_l = \sum_{l=1}^{\infty} (l+1) \sum_{m=1}^{l} [(g_l^m)^2 + (h_l^m)^2]. \tag{3}$$

Spectra of the magnetic fields due to the core and the crust inevitably overlap, and can each cause contamination of

both studies of the core field and of the crustal field. In Fig. 1(a) we show the power spectrum of the field computed from several recent models of the magnetic field, namely models M07AV6 of Cain *et al.* (1989), MGST(10/81) of Langel & Estes (1982) and M040589 (J. C. Cain, unpublished). The usual interpretation of this figure (Lowes 1974) is that below the 'knee' in the curve the power is due to sources in the core, and above the knee the sources are in the crust. For model M07AV6 the break appears at roughly degree 15. This interpretation of the spectra is entirely *ad hoc* and, whilst plausible, does make strong assumptions about the form of the spectra which originate in the core and crust. Is there any way to rule out the possibility that, for example, all the observed signal originates in the core? One such method does exist, based on the so-called 'heat-flow bound' (Parker 1972; Gubbins 1975; Backus 1988a). This bound uses the fact that the core magnetic field is sustained by currents which cause Ohmic dissipation within the core which must not exceed the heat observed to be flowing out of the earth's surface [if the earth is in a steady state and geophysically reasonable core temperatures are chosen so that the ratio of dissipation rate to heat flux is less than unity; see Hewitt, McKenzie & Weiss (1975) and Backus (1975)]. Only the poloidal magnetic field is observable at the core surface, but for such a field it is possible to calculate the field configuration within the core which leads to the minimum rate of Ohmic heat production Φ. Then if σ is the core productivity, μ_0 is the permeability of free space and c is the core radius we find (Gubbins 1975)

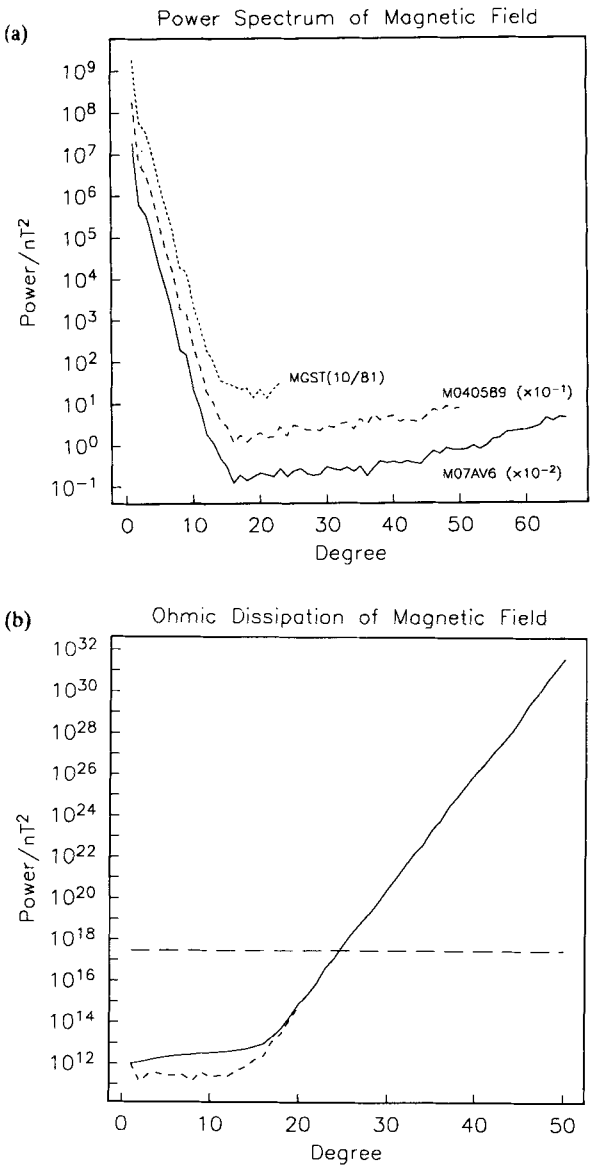

Figure 1. Contributions by harmonic degree to two norms of the magnetic field, as determined by the satellite *Magsat*. (a) Power spectrum versus harmonic degree for models MGST(10/81) (Langel & Estes 1982), M040589 (J. C. Cain, unpublished) and M07AV6 (Cain *et al.* 1989). The last two spectra have been multiplied by factors of 10^{-1} and 10^{-2} for clarity. (b) Minimum rate of heat production from Ohmic dissipation within the core if all harmonics of the field observed at the earth's surface were due to the field in the core. The dotted line is the contribution to Q_{hb} (see equation 5) from each degree up to $l = 20$, and the solid line is the cumulative value of Q_{hb} as each spherical harmonic degree is included, using model M07AV6 of Cain *et al.* (1989). The horizontal line is the value of $Q_{hb} = 3 \times 10^{17}$ nT^2 for the parameters adopted in the text.

$$\Phi = \frac{4\pi c}{\mu_0^2 \sigma} \sum_{l=1}^{\infty} \frac{(l+1)(2l+1)(2l+3)}{l} \times \left(\frac{a}{c}\right)^{2l+4} \sum_{m=1}^{l} [(g_l^m)^2 + (h_l^m)^2]. \quad (4)$$

Now, defining

$$Q_{hb}(\mathbf{B}) = \Phi \sigma \mu_0^2 / 4\pi c \quad (5)$$

and taking $\sigma = 3 \times 10^5$ S m^{-1}, $\mu_0 = 4\pi \times 10^{-7}$ H m^{-1}, $c =$ 3485 km and $\Phi = 3 \times 10^{13}$ W (the observed heat flow out of the earth's surface) gives a maximum permissible value of $Q_{hb} = 3 \times 10^{17}$ nT^2 (Backus 1988a). In Fig. 1(b) we show the cumulative value of Q_{hb} as each spherical harmonic degree is added for model M07AV6. Clearly at degree 25 the heat-flow bound is exceeded; this cannot preclude harmonics above degree 25 being present in the core field as contamination is sure to have occurred, but it does prove decisively that all the signal cannot originate in the core (provided our assumptions are not egregious). This motivates an examination of possible sources of field which originate in the crust and which are capable of reproducing, at least asymptotically, the observed power spectrum.

3 DETERMINISTIC CHARACTERIZATION

This section considers effects of induced magnetization. In particular we examine the possibility that simple deterministic models, which are based on physical considerations independent of magnetic data, can account for the observed power spectrum. The models we shall discuss are intuitively appealing and their verification would be important in geomagnetism because they would allow the removal of much of the crustal field which at present contaminates studies of the core field.

Meyer and colleagues first suggested that the high-degree power spectrum was due to induced magnetization resulting from regional differences in magnetic susceptibility of crustal rocks (Meyer *et al.* 1983, 1985; Hahn *et al.* 1984). They construct a global model of the susceptibility of the crust, based on geological information, and show that the external

field which results from the field induced in the crust by an internal dipole reproduces the observed spectrum extremely well. More recently, Counil, Achache & Cohen (1989) have suggested a simplification of this model. They suggest that the induced field is well approximated by that which results from a simple contrast in vertically integrated susceptibility between continents and oceans. Both models therefore describe the spatial distribution of susceptibility and require only an internal field model for their effects to be computed.

To compute the induced field we use standard results from potential theory. The induced field $\Delta\mathbf{B}$ is given by $\Delta\mathbf{B} = -\nabla\Phi$, where

$$\Phi(\mathbf{r}_j) = \int_V \mathbf{H}_j(s) \cdot \mathbf{M}(\mathbf{s})\, d^3\mathbf{s} \tag{6}$$

and $\mathbf{H}_j(\mathbf{s})$ (the Green's function for the potential) is given by

$$\mathbf{H}_j(\mathbf{s}) = \mathbf{H}(\mathbf{r}_j, \mathbf{s}) = \frac{\mu_0}{4\pi} \nabla \frac{1}{|\mathbf{r}_j - \mathbf{s}|} \tag{7}$$

where μ_0 is the permeability of free space, $4\pi \times 10^{-7}\,\mathrm{H\,m^{-1}}$.

Now to first order in the susceptibility χ the magnetization $\mathbf{M}$ is given by

$$\mu_0\mathbf{M} = \chi\mathbf{B}_i = -\chi\nabla V_i \tag{8}$$

where $\mathbf{B}_i$ is the internal magnetic field described as the gradient of the internal potential V_i. Thus the induced potential Φ is given by

$$\Phi(\mathbf{r}_j) = -\mu_0^{-1} \int_V \chi\mathbf{H}_j(\mathbf{s}) \cdot \nabla V_i\, d^3\mathbf{s}. \tag{9}$$

For a particular susceptibility distribution and internal field model, Appendix A shows how the induced potential Φ can be calculated as a spherical harmonic expansion equivalent to equation (1) but with new coefficients $\{i_l^m; j_l^m\}$ instead of the $\{g_l^m; h_l^m\}$ of the main field.

Adopting the suggestion of Counil *et al.* (1989), we have computed the induced field which results from a difference in vertically integrated magnetic susceptibility between the continents and oceans. A theorem due to Runcorn (1975) shows that only the difference in susceptibility is relevant, because the field induced by a shell of constant susceptibility vanishes. Therefore we adopt a model of susceptibility where

$$\chi(\theta, \phi) = \begin{cases} \chi_0 & \text{if } (\theta, \phi) \in C, \quad a \le r \le b \\ 0 & \text{if } (\theta, \phi) \notin C \end{cases} \tag{10}$$

where C represents the continents and $d = a - b$ is the depth of the Curie isotherm. Appendix A gives an accurate method of calculating the spherical harmonic representation of χ; the power spectrum of this representation to degree 70 is shown in Fig. 2(a). Fig. 2(b) shows the power spectrum of the field induced by the continent distribution to degree 60 when the vertically integrated susceptibility $\chi_0 d = 1.4$ km, and also the induced field of model CRST-70-F-22-22- of Hahn *et al.* (1984) to degree 35. Both show a flat spectrum beyond roughly degree 10. Note the peaks in both spectra at degrees 4 and 6, a consequence of the coupling between an internal dipole and the peaks in the continent function at degrees 3 and 5 (a consequence of the predominance of land in the northern hemisphere) in Fig. 2(a).

The spectra of both representations certainly reproduces that seen in the power spectra of magnetic field models (Fig. 2c). However, since these models make definite deterministic predictions regarding the magnetic field, to be substantiated both models must not only reproduce the power spectra but must stand up to tests against the original

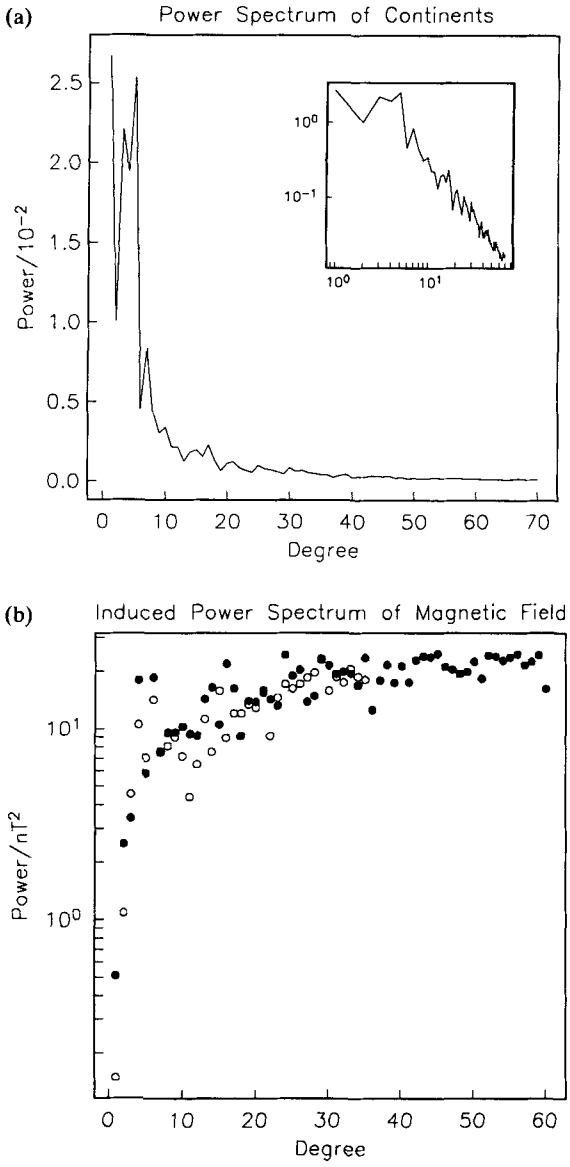

Figure 2. (a) Power spectrum of the spherical harmonic representation of the continent function. Note the large contributions from the odd degrees, especially $l = 1$, 3, 5. Inset is the same on a log–log scale. (b) Power spectrum of magnetic field induced by the continent function and an internal source (filled circles) when $\chi_0 d = 1.4$ km. Also plotted is the spectrum for the model of the induced field CRST-70-F-22-22- of Hahn *et al.* (1984) (open circles). Note the peaks at degrees 4 and 6, a consequence of the coupling between an internal dipole and the peaks in the continent function at degrees 3 and 5 in (a). (c) The same spectra as in (b) but plotted along with model M07AV6 of Cain *et al.* (1989). Beyond $l = 10$ the induced power spectrum is approximately flat, in accord with the observed power spectrum.

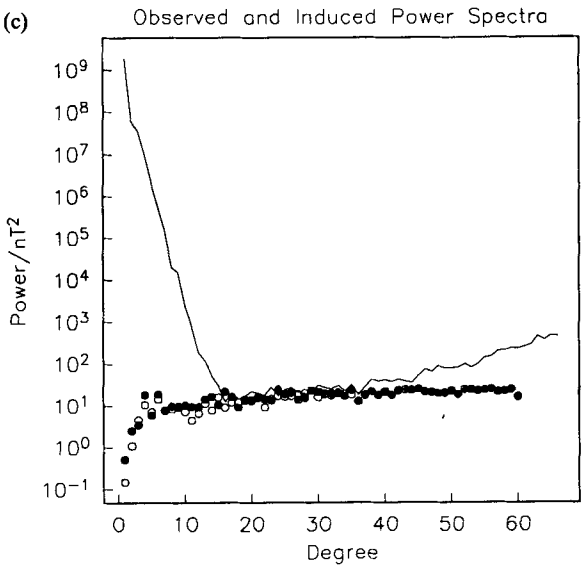

Figure 2. (*continued*)

magnetic data. The induced signal (if present) below degree 15 is small in comparison to the core field, and must be contained in any model of the field which is derived from satellite data. Therefore the primary 'data' for such a test must be the residuals to a field model such as M07AV6 (Cain *et al.* 1989) truncated at or near degree 15; we can then assess whether the induced models above degree 15 represent in any way the observed signal. To gain acceptability such a deterministic model must reduce the variance of a large set of such data.

We have carried out such a test for both the models of Hahn *et al.* (1984) and the continent model and the results are shown in Figs 3(a) and 3(b). Almost 50 000 *Magsat* residuals from model M07AV6 truncated at degree 15 were used, after corrections for secular variation from the model of Bloxham & Jackson (1989) and external fields from the model of Langel & Estes (1985). Histograms of the residuals in each of the measured field components show that the residuals conform well to a Gaussian distribution, and so the chi-squared statistic is a good measure of the fit to the data. In fact we use the root mean square residual or misfit σ where

$$\sigma^2 = 1/N \sum_{i=1}^{N} (\gamma_i - \tilde{\gamma}_i)^2 \qquad (11)$$

and $\tilde{\gamma}_i$ is an appropriate prediction obtained using (9). Figs 3(a) and (b) plot the variation in misfit with variation in $\chi_0 d$. Unfortunately neither model appears to reduce the variance significantly, and the smallest misfits occur at values of susceptibility which no longer reproduce the power spectra (i.e. the values are too small to account for most of the internal signal beyond degree 15). For the model of Hahn *et al.* (1984) the minimum misfit occurs when it is scaled by a factor of approximately 0.2 in each of the field components. Hahn *et al.* use typical values of vertically integrated susceptibility of $\chi_0 d \sim 75$ m for much of the oceans (corresponding to susceptibilities of $\chi_0 \sim 1.5 \times 10^{-2}$), and $\chi_0 d$ ranges from 500 m to over 1.6 km for continents. On the basis of this study it would appear that such a large contrast in ocean/continent susceptibility is not upheld. For the

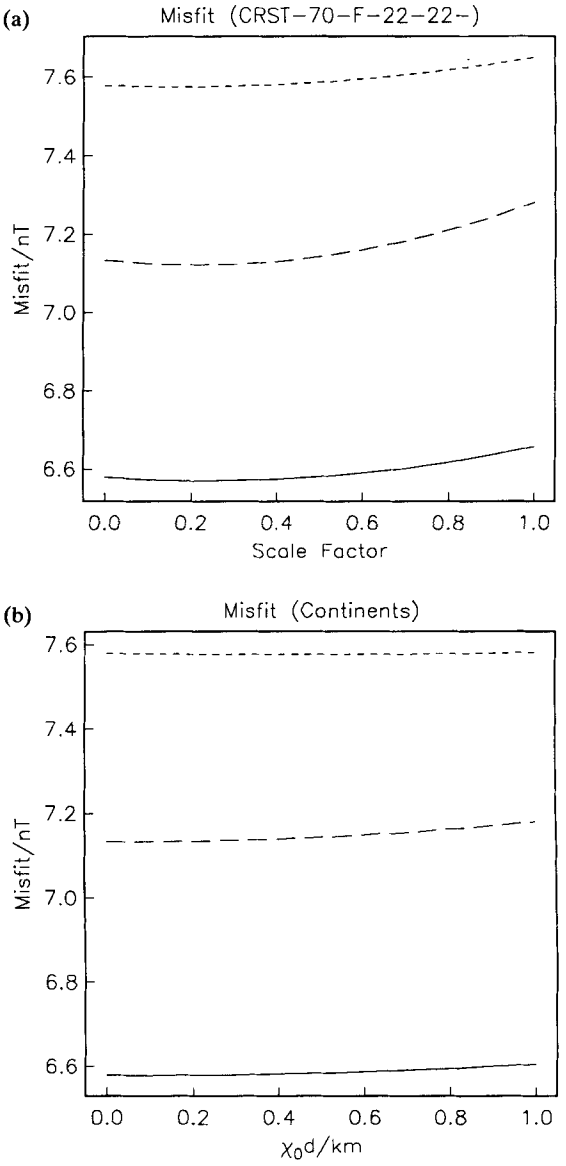

Figure 3. (a) Change in misfit between predictions from continentally induced magnetization and *Magsat* residuals as a function of continent/ocean contrast in vertically integrated susceptibility $\chi_0 d$. The residuals are those remaining after subtraction of the Cain *et al.* (1989) model of the main field ($l \leq 15$), and the predictions are based on degrees $l > 15$. A contrast of $\chi_0 d \approx 1.4$ km would be required to account for the power spectrum. Solid line is *X*, short dash *Y*, long dash *Z*. (b) As in (a) but using the model CRST-70-F-22-22- of Hahn *et al.* (1984) and changing the amplitude of the predictions. A scale factor of 1 represents the original model of Hahn *et al.* which reproduces the power spectrum.

continent model the best fitting value for $\chi_0 d$ is different for different field components: *X* suggests $\chi_0 d \sim 40$ m, whereas *Y* suggests $\chi_0 d \sim 200$ m. This result is not altogether unexpected: after subtraction of the first few degrees of the continent function, the resulting model represents mostly an edge effect, but it is almost impossible to discern such a signal in *Magsat* data. The simplicity of the ocean/continent model of Counil *et al.* (1989) is appealing, because it is effectively a one-parameter model, but it does not appear to

represent a large proportion of the signal attributable to the crust. More complex models could be constructed [the model of Hahn *et al.* (1984) is extremely detailed], but as our interest is primarily in the core field, an alternative approach presents itself, namely a stochastic representation of the crust. This is discussed in the next section.

4 STOCHASTIC CHARACTERIZATION

Any attempt to model the magnetic field requires first the specification (at least approximately) of the probability density function (pdf) of the errors which contaminate the data. This section is concerned with this specification, when the presence of the crustal field is considered. If $\boldsymbol{\gamma}$ is a data vector composed of $\{\gamma_i\}$, $i = 1, N$, then for large N the pdf of the corresponding errors $\mathbf{e}$ due to many random sources tend, by the Central Limit theorem, towards a Gaussian distribution, written

$$p(\mathbf{e} \mid \mathbf{m}) = [(2\pi)^N \det \mathbf{C}_r]^{-1/2} \exp\{-\tfrac{1}{2}\mathbf{e}^T\mathbf{C}_r^{-1}\mathbf{e}\} \tag{12}$$

where $\mathbf{C}_r$ is the (diagonal) covariance matrix of random errors and $\mathbf{m}$ is the true earth model. If we consider errors due to crustal magnetization to be independent and Normally distributed with covariance $\mathbf{C}_c$, then the final pdf is also a Gaussian of the form (12) with covariance $\mathbf{C}_e = \mathbf{C}_c + \mathbf{C}_r$ (e.g. Tarantola 1987, p. 158).

To consider the remanent crustal contribution $\mathbf{C}_c$ to the full covariance $\mathbf{C}_e$ we follow an idea of Parker (1988) closely. In his study of seamount magnetization, he found that seamount magnetic anomaly data could be modelled much more successfully, and a more consistent palaeopole position constructed, if he allowed the modelling to include a statistically random source of magnetization *within the seamount* which would be viewed as noise. A similar scenario occurs with satellite data, because the long-wavelength core field, originating at $r = c$, is contaminated by shorter wavelength noise which originates mostly at the earth's surface, $r = a$. Adjusting the arguments of Parker for the present case, if $e_i^{(\eta)} = e^{(\eta)}(\mathbf{r}_i)$ is the error in a field measurement of component η at position $\mathbf{r}_i$ due to the magnetization of the crust $\mathbf{M}(\mathbf{s})$, then the errors are related to $\mathbf{M}$ by

$$e_j^{(\eta)} = \int_V \mathbf{G}_j^{(\eta)}(\mathbf{s}) \cdot \mathbf{M}(\mathbf{s})\, d^3\mathbf{s} \tag{13}$$

where $\mathbf{G}_j^{(\eta)}(\mathbf{s}) = \mathbf{G}^{(\eta)}(\mathbf{r}_j, \mathbf{s})$ is the Green's function for the problem, $\mathbf{r}_j$ is the observation point, and $\mathbf{s}$ is any vector within the volume of the crust V. Fig. 4 shows schematically the geometry and notation used for the problem. In reality, the magnetic layer, of depth d, is extremely thin ($d/a \sim 5 \times 10^{-3}$ for the earth).

In the case of measurements of orthogonal components of the field X, Y, and Z in the northward, eastward and downward directions, the Green's functions are

$$\mathbf{G}^{(\eta)}(\mathbf{r}_j, \mathbf{s}) = -\frac{\mu_0}{4\pi}\hat{\boldsymbol{l}}_j^{(\eta)} \cdot \nabla_{\mathbf{r}_j}\nabla_{\mathbf{s}}\frac{1}{|\mathbf{r}_j - \mathbf{s}|}$$

where

$$\hat{\boldsymbol{l}}_j^{(\eta)} = \begin{cases} -\hat{\boldsymbol{\theta}}, & \eta = X \\ \hat{\boldsymbol{\phi}}, & \eta = Y \\ -\hat{\mathbf{r}}, & \eta = Z \end{cases} \tag{14}$$

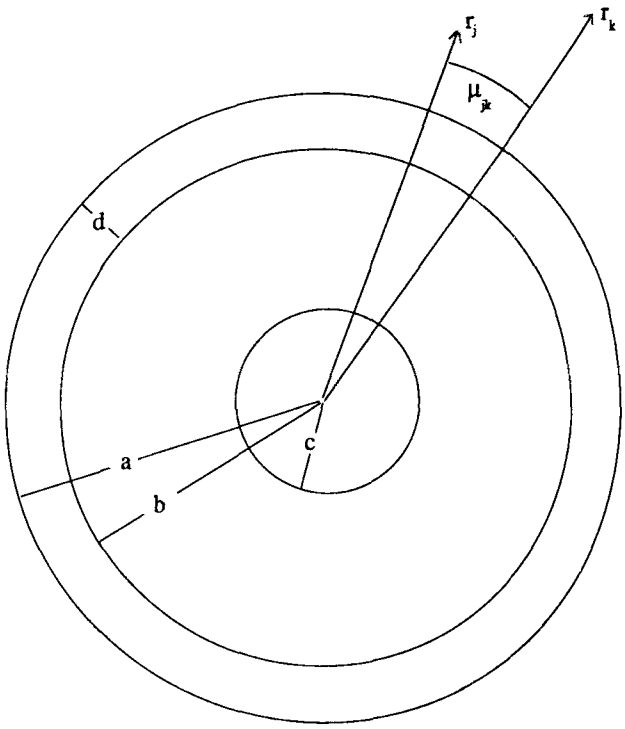

Figure 4. Schematic figure showing the geometry and notation used in the text. The earth's radius is a, the core radius is c and the depth of the magnetic shell is $d = a - b$. Two satellite positions $\mathbf{r}_j$ and $\mathbf{r}_k$ are separated by a (great circle) angular distance of μ_{jk}.

and where $\nabla_{\mathbf{r}_j}$ means differentiation with respect to $\mathbf{r}_j$. The Green's function for the crustal error in measurements of total field strength F can be found in Appendix B.

The errors have covariance

$$\begin{aligned}[\mathbf{C}_c]_{jk}^{(\eta\nu)} &= E\{e_j^{(\eta)}e_k^{(\nu)}\} \\ &= E\left\{\int_V \mathbf{G}_j^{(\eta)}(\mathbf{s}) \cdot \mathbf{M}(\mathbf{s})\, d^3\mathbf{s} \int_{V'} \mathbf{G}_k^{(\nu)}(\mathbf{s}') \cdot \mathbf{M}(\mathbf{s}')\, d^3\mathbf{s}'\right\} \\ &= \int_V \int_{V'} \mathbf{G}_j^{(\eta)}(\mathbf{s}) \cdot E\{\mathbf{M}(\mathbf{s})\mathbf{M}(\mathbf{s}')\} \cdot \mathbf{G}_k^{(\nu)}(\mathbf{s}')\, d^3\mathbf{s}\, d^3\mathbf{s}'\end{aligned} \tag{15}$$

where $\mathbf{s}$ and $\mathbf{s}'$ both lie within the magnetized volume, E stands for expectation and integration and expectation have been freely exchanged.

To make progress, the form for the covariance tensor $\mathbf{M} = E\{\mathbf{M}(\mathbf{s})\mathbf{M}(\mathbf{s}')\}$ must be specified. We begin by assuming the crustal magnetization to be a stationary, zero-mean, Gaussian random process. This is a very different assumption to that of most other workers who treat the crust as a deterministic system whose magnetic features can be recovered (e.g. Ritzwoller & Bentley 1982; LaBrecque & Raymond 1985), but then our aims are different: our interest is in the core field. From the linearity of equation (13), if $\mathbf{M}(\mathbf{s})$ is a stationary, zero-mean, Gaussian random process, then the residuals $e_j^{(\eta)}$ are samples from one also, and their pdf is completely specified by the covariance matrix. Stationarity implies that the statistics of $\mathbf{M}(\mathbf{s})$ are independent of position vector $\mathbf{s}$. This type of model has been used in applications other than the cited work of Parker; for example the modelling of seafloor topography by Goff & Jordan (1988).

In Parker's application, the random part of the seamount magnetization plays the same role as the crustal magnetization **M**. Parker argued that **M** would be purely uncorrelated at different positions, and in different components: thus the components of **M** at two positions average zero, except in the trivial case of identical components at the same site. This is the simplest possible scenario, but seems very reasonable, and even with this assumption, Parker's results were impressive. From this assumption, the correlation tensor becomes

$$E\{\mathbf{M}(\mathbf{s})\mathbf{M}(\mathbf{s}')\} = \beta^2 \mathbf{I}\delta(\mathbf{s}-\mathbf{s}') \tag{16}$$

where **I** is the identity matrix, $\delta(\mathbf{s})$ is the Dirac delta function, and β^2 is a constant. Equation (15) then becomes

$$[\mathbf{C}]_{jk}^{(\eta\nu)} = \beta^2 \int_V \mathbf{G}_j^{(\eta)}(\mathbf{s}) \cdot \mathbf{G}_k^{(\nu)}(\mathbf{s})\, d^3\mathbf{s} \tag{17}$$

$$= \beta^2 \Gamma_{jk}^{(\eta\nu)} \tag{18}$$

which is just a multiple of the standard Gram matrix Γ of the data kernels.

The true length-scale for correlations must, in reality, be longer than the infinitesimal one assumed; however, provided it is very much smaller than the scale length of variations in the Green's function, then (16) will be a good approximation. As Parker points out, if a finite length-scale of correlation is included, the dimensionality of the integrals is increased threefold, and the results become significantly more complicated. Also, this assumption leads to the minimum possible correlation between the residuals; in reality the residuals must be more correlated than this, but at least we have improved over the usual assumption of completely uncorrelated residuals.

Is this correlation function reasonably consistent with our knowledge of crustal magnetization? Parker & Daniel (1979) note that vertical sections of drilled seafloor lose almost all correlation in magnetization after about 10 m. Therefore our approximation of infinitesimal vertical length-scale is probably an adequate one. Except in areas corresponding to quiet periods in the reversal sequence, oceanic stripes suggest that at the most the correlation length perpendicular to the spreading axis is about 20 km. Parallel to the spreading axis the correlation length-scale must be longer, although transform faults probably restrict this.

Remanent magnetization can only occur at temperatures above the Curie temperature, T_c. The depth to the Curie isotherm depends on the particular mineral assemblage, and must also be shallower in areas of high heat flow. Curie temperatures range from below 300°C to over 550°C (Mayhew, Johnson & Wasilewski 1985), though the higher value is more representative. Mayhew *et al.* also identify the Moho with the 'magnetic bottom' in their terminology. For simplicity we take the depth to be constant; the precise value does not affect the conclusions profoundly. The calculations we have performed have taken the depth to the Curie isotherm d to be 35 km, a figure suitable for continental crust. In fact we find that the results are insensitive to a shallower value for d (of say 5 km for oceanic crust), provided β^2 is adjusted appropriately [see the discussion below equation (23)].

4.1 Correlation functions for satellite observations

Details of the integrations needed to find the correlation functions (i.e. equation 18) for magnetic field measurements are set out in Appendix B. It is shown there that the covariance of errors e in field components η and ν at positions $\mathbf{r}_i$ and $\mathbf{r}_j$ due to the crust is given by

$$E\{e_i^{(\eta)}e_j^{(\nu)}\} = a^2 k(\beta)\hat{\mathbf{l}}_i^{(\eta)} \cdot \nabla_{\mathbf{r}_i}\hat{\mathbf{l}}_j^{(\nu)} \cdot \nabla_{\mathbf{r}_j} \sum_{l=0}^{\infty} \frac{l}{2l+1} \times \rho^{l+1} P_l(\mu)\left[1 - \left(\frac{a-d}{a}\right)^{2l+1}\right] \tag{19}$$

where E stands for expectation, the vectors $\hat{\mathbf{l}}_i^{(\eta)}$ are defined in (14), P_l is a Legendre polynomial of degree l, μ is the angular separation of the two points, d and a are the depth of the magnetized layer and the earth's radius respectively, and $\rho = a^2/r_i r_j$. The amplitude of the covariance depends on the factor $k(\beta) = \beta^2\mu_0^2/4\pi a^3$, which is proportional to the size of β^2 in (16). Our task is to find an appropriate amplitude for the covariance.

Equation (19) shows that the errors are derived from a correlated potential of the form

$$E\{\phi_m(\mathbf{r}_j)\phi_m(\mathbf{r}_k)\} = a^2 k(\beta) \sum_{l=0}^{\infty} \frac{l}{2l+1} \times \rho^{l+1} P_l(\mu)\left[1 - \left(\frac{a-d}{a}\right)^{2l+1}\right]. \tag{20}$$

In terms of a conventional spherical harmonic representation of the form (1), we can find the covariance of the Gauss coefficients which represent the crustal field. Using the orthogonality of the spherical harmonics, we find

$$E\{\alpha_l^m \gamma_{l'}^{m'}\} = k(\beta)\frac{l}{2l+1}[1-(1-\epsilon)^{2l+1}]\delta_{ll'}\delta_{mm'}\delta_{\alpha\gamma} \tag{21}$$

where $\epsilon = d/a$, $\delta_{ll'}$ is the Kronecker delta and α_l^m, γ_l^m stands for either g_l^m or h_l^m. Therefore the equivalent Gauss coefficients are uncorrelated. The predicted power spectrum depends only on the spherical harmonic degree l, so using the notation of equation (3) we find

$$R_l = l(l+1)k(\beta)[1-(1-\epsilon)^{2l+1}]. \tag{22}$$

The small and large l limits are

$$R_l = \begin{cases} l(l+1)(2l+1)\sigma^l \epsilon k(\beta), & l \ll 1/\epsilon \\ l(l+1)k(\beta), & l \to \infty \end{cases} \tag{23}$$

where $\sigma = \exp(-\epsilon)$. For $d = 35$ km, $\epsilon \sim 5 \times 10^{-3}$ and the small l expression in (23) is good for $l \ll 180$; different values of d can be accommodated by a change in the value of $k(\beta)$. We can now choose $k(\beta)$ appropriately to give agreement between the measured and calculated spectra: note that the shape of the spectrum is completely specified (because of the correlation function adopted) and only the amplitude is required. We find $k(\beta) = 0.0625\,\text{nT}^2$ gives an adequate fit to the spectrum beyond $l \approx 14$, where contamination by the core field is probably small, and we adopt this value for the rest of the paper. Fig. 5 shows the predicted power as a function of l compared to the observed spectrum at a typical satellite altitude of 400 km and at the earth's surface (although at the earth's surface the spectrum does not converge and of course the real one does). The

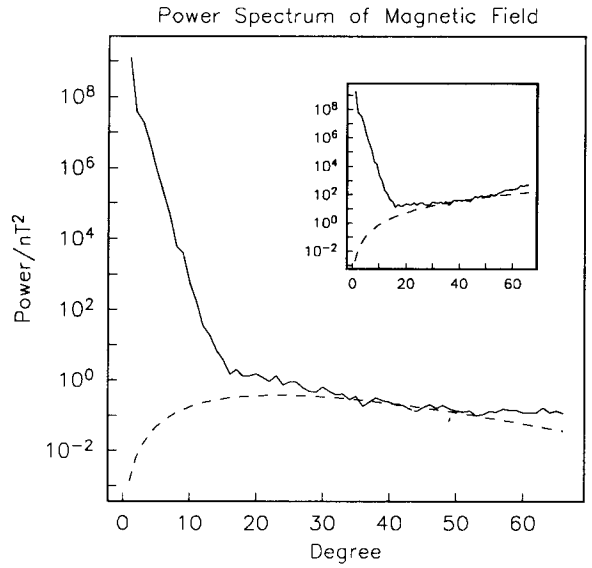

Figure 5. Predicted power spectrum of stochastic remanent magnetization model compared to that of model M07AV6 of Cain *et al.* (1989) at a satellite altitude of 400 km. The thickness of magnetized crust is taken as 35 km, and $k(\beta) = 0.0625\ \mathrm{nT}^2$ (see text for definition). Inset is the same at the earth's surface.

agreement is reasonable between degrees 30 and 50; beyond $l = 50$ the measured spectrum appears to rise, which may or may not be a real effect; there remains the possibility of corruption of the spectrum by noise because of the approximate method of inversion used by Cain *et al.* (1989).

Figure 6(a–d) shows the correlation functions for different field components as a function of separation, at an altitude of 400 km typical of *Magsat,* with a magnetization depth of 35 km and one point on the equator. Correlations persist over separations of up to 15°, or roughly 1500 km.

The covariance between two Z components is independent of their positions, and depends only on their separation; the covariance between other field components depends on the azimuth (measured clockwise from north) of one position from the other, and on their position on the sphere. This dependence is a consequence of the fact that the field components X, Y, and Z are defined in a spherical coordinate system in which field components are only locally orthogonal (i.e. non-Euclidean). Note that the covariances are zero in the case of two orthogonal field components being measured at the same point (corresponding to $\mu_{ij} = 1$ in Appendix B).

Figure 6(a and b) shows the covariances for field components $\{ZZ\}$ and $\{YY\}$. The covariance of $\{YY\}$ at azimuth 0° decreases monotonically to zero by a separation of about 15°; at azimuth 90°, by contrast, negative correlation occurs from separations of about 4° onwards. For $\{ZZ\}$ at all azimuths negative correlation occurs from separations above approximately 6°. Fig. 6(c and d) shows the covariances of the off-diagonal members of the tensor; at zero separation these field components are completely uncorrelated, as expected. The $\{YZ\}$ correlation appears to peak at a separation of roughly 3°. The variation of $\{XY\}$ is interesting since at azimuths of both 90° and 0° these field components are uncorrelated. In between, the correlations are non-zero, and at an azimuth of 45° the field components

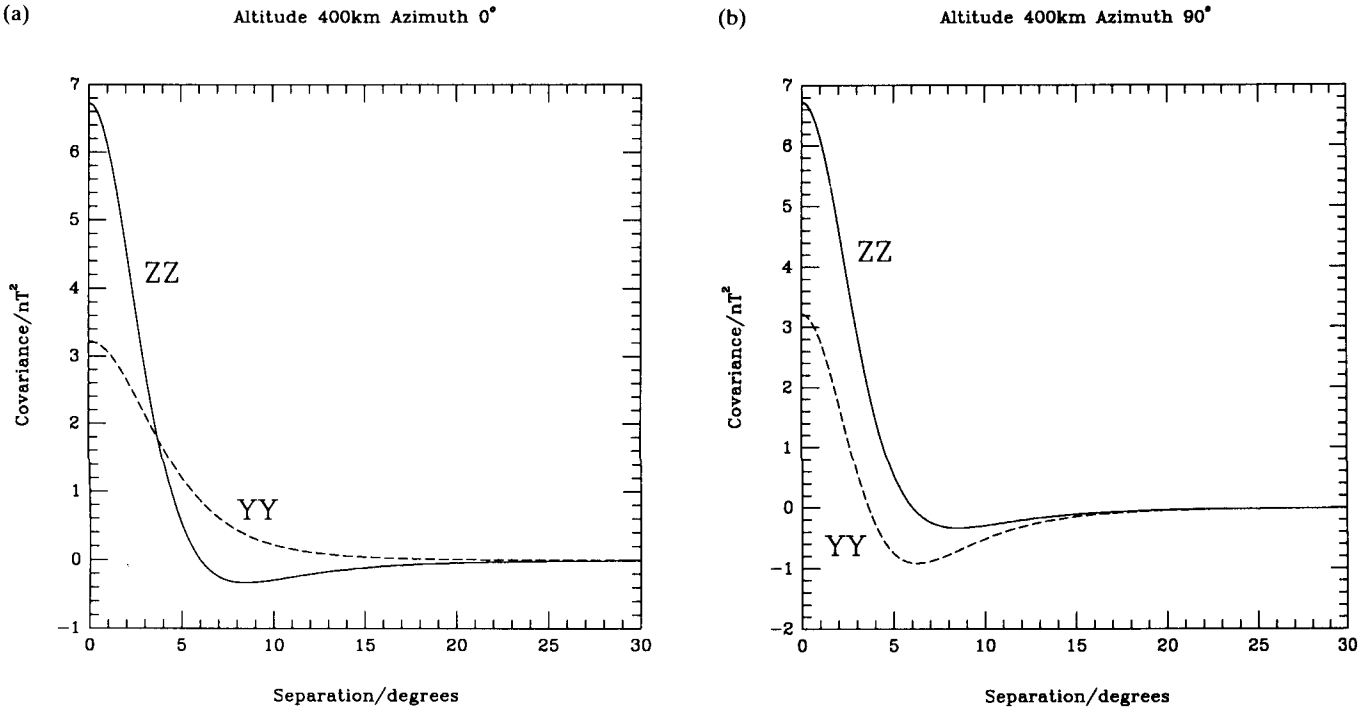

Figure 6. Correlation of different field components at satellite altitude given by $\mathbf{C}_c$, as a function of the angular separation of the observing sites and for different azimuths (measured clockwise from north) when one point is on the equator. The altitude is 400 km, and the crustal parameters are as in Fig. 5. (a) and (b) show the covariance of $\{ZZ\}$ and $\{YY\}$ at azimuths 0° and 90°. The covariance of $\{ZZ\}$ is independent of azimuth. (c) and (d) show the covariance of $\{XY\}$ and $\{YZ\}$ at azimuths 45° and 90°. At azimuth 0° both are uncorrelated.

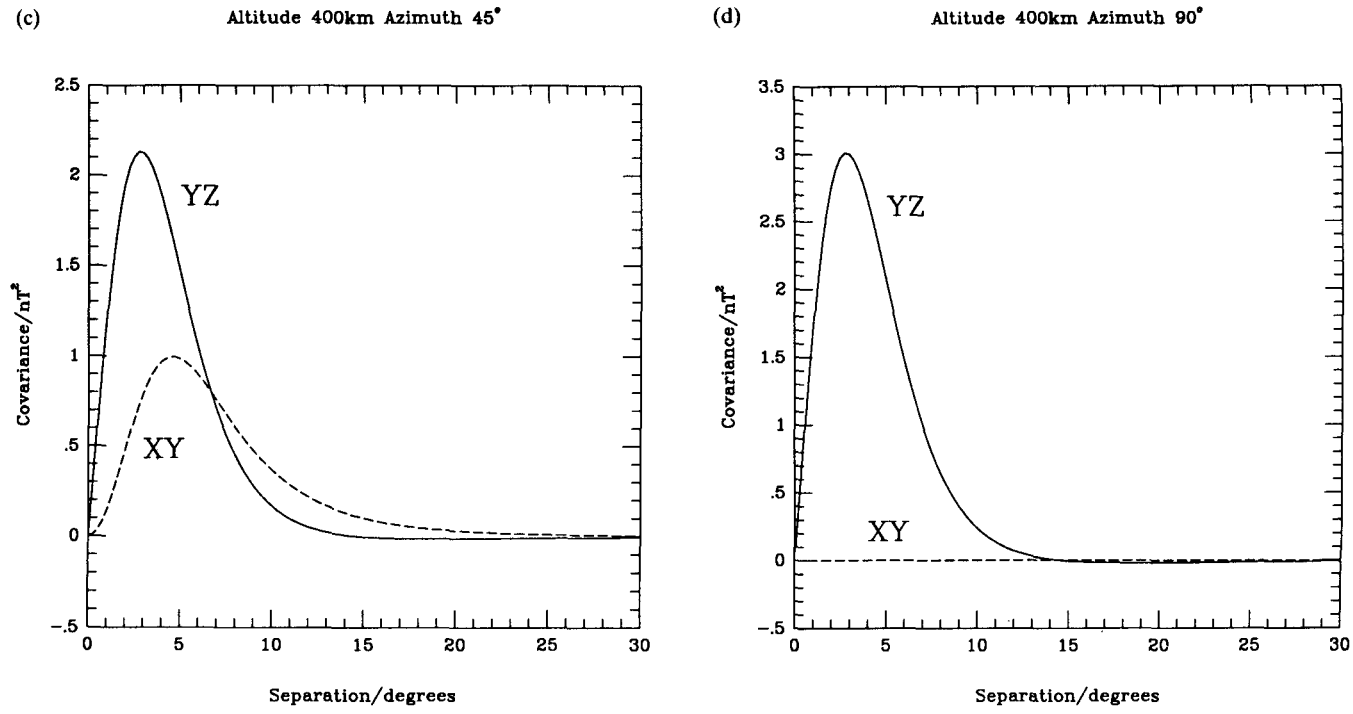

Figure 6. (*continued*)

appear to have the longest range correlation of any pair of field components.

Consider now the special case $\mathbf{r}_i = \mathbf{r}_j$ (i.e. two measurements at the same observation point). Fig. 6(c and d) clearly shows that different field components are uncorrelated at the same position, so only the covariance of one field component with itself (i.e. its variance) need be considered. Fig. 7 shows the predicted dependence of variance in observations of X, Y and Z with altitude. For typical *Magsat* altitudes, the predicted variances change by a factor of 6 between 350 and 550 km. Note that the variances in X are equal to those in Y (since both are measurements of horizontal field at the same position, which cannot differ if the crustal field is isotropic as we have assumed), and that the variances in Z are approximately twice those in X or Y. The variances for F measurements must necessarily lie between the lines for the Z and X variances, since these depend on the local direction of the main field $\mathbf{B}_0$.

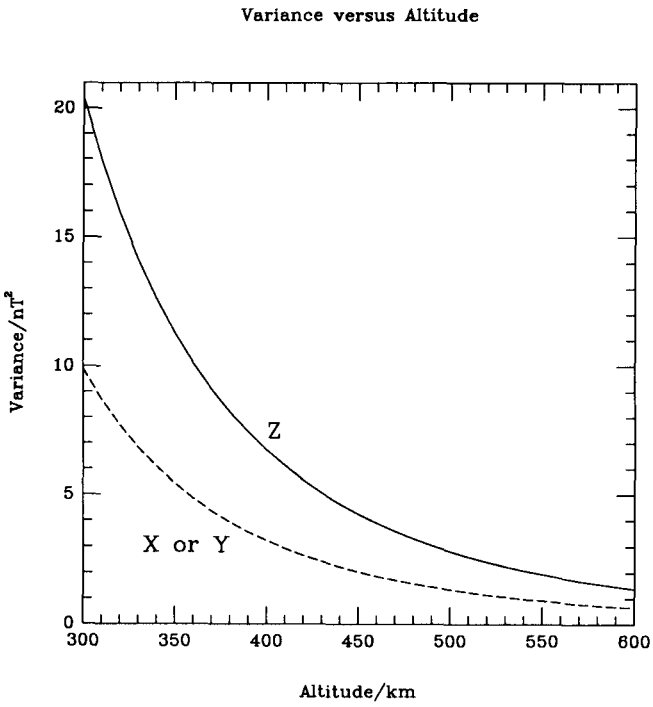

Figure 7. Predicted variance of crustal field versus altitude for field components Z (solid line) and X,Y (dashed line). Crustal parameters as in Fig. 5.

The above discussion shows that previous studies of the core field which have treated each datum as independent are in error not only because of the ignorance of correlation in the data but also because the expected variance in Z data due to the crust is approximately twice as large as that in X or Y data.

5 CONCLUSIONS AND DISCUSSIONS

We have considered two possible representations of the effect of the crust on satellite observations of the core field, namely as deterministic and stochastic effects. The first, which is mainly due to the difference in susceptibility between oceans and continents, requires that the vertically integrated susceptibility $\chi_0 d \approx 1.4$ km in order to account for the majority of the observed crustal spectrum. However, the data only seem to (weakly) suggest $\chi_0 d \approx 0.1$ km, which gives a contribution to the power spectrum of less than one hundredth of that required. The model of Hahn *et al.* (1984), whilst fitting the data better, also requires the amplitude of the susceptibility contrast to be reduced.

For the stochastic part we have shown that subject to our assumption that the crust can be thought of as a stationary,

isotropic, zero-mean random process, the averaging property of the appropriate Green's function leads to significant correlation in the data even when the magnetization of the crust is completely uncorrelated in space. Correlations appear to be significant over angular separations of up to 15°. The information on the correlation in the data due to the crust which is contained in the matrix $\mathbf{C}_c$ is important in an inversion for the core field because when used in combination with the random covariance $\mathbf{C}_r$ it determines the linearly independent combinations of data which should be fit by the model.

Recently Langel *et al.* (1989) (hereinafter LES) considered the same problem of crustal contamination in the context of deriving more rigorous error estimates on Gauss coefficients, although they consider other effects such as secular variation errors and ionospheric fields in addition. Since the methods and results presented here differ from those of LES it is worth highlighting these differences. The treatment of the crustal field of LES is based on an interpretation of the power spectrum (3). They note that an empirical description of the power spectrum of Fig. 1(a) which agrees reasonably with the observations is that for $l \lesssim 13$,

$$R_l = R_i(p_i)^l \tag{24}$$

whilst for $l \gtrsim 14$,

$$R_l = R_c(p_c)^l. \tag{25}$$

For the power in $l \gtrsim 14$, Langel & Estes (1982) find $R_c = 37.1$ nT, $p_c = 0.974$, whilst Cain *et al.* (1989) find $R_c = 19.1$ nT, $p_c = 0.996$. LES adopt an estimate of the spectrum of the crustal field of the form (25) but rather than adopting any of the measured values for R_c or p_c, they adopt $R_c = 20$ nT, $p_c = 0.9999387$ to give agreement with the rms sizes of crustal anomalies at observatories inferred from the misfit to satellite models of the core field; they also extrapolate the spectrum to the regime $l \lesssim 14$ where it is masked by the core field. LES use their adopted values to estimate the covariance of the Gauss coefficients of the crustal field from the power spectrum: they assume

$$E\{\alpha_l^m \gamma_{l'}^{m'}\} = R_l/[(2l+1)(l+1)]\delta_{ll'}\delta_{mm'}\delta_{\alpha\gamma} \tag{26}$$

where E stands for expectation, $\delta_{ll'}$ is the Kronecker delta and α_l^m, γ_l^m stand for either g_l^m or h_l^m. This assumes that there is no correlation between the Gauss coefficients representing the crustal field; we find this to be so in the theory described here (equation 21), but independence is not a necessity [for example, Constable & Parker (1988) find correlation between the coefficients g_1^0 and g_2^0 of the main field on the palaeomagnetic time-scale].

The resulting covariance functions of LES are shown in Fig. 8(a and b) for altitude 400 km and azimuth 90°, which should be compared with Fig. 6(b and d). The amplitude and length-scale of the figures are predictably different, given the different assumptions. The theory of LES shows significant correlation at extremely large separations, in comparison to the length-scales (~15°) reported here. To show the disparity in amplitude, consider a single measurement of the vertical component of field: the standard deviation of the measurement is predicted to be 8.2 nT, in contrast to 2.6 nT predicted by our theory. Clearly the estimates of the power in the crustal field at low spherical harmonic degree crucially affect the estimate of covariance in the data, and the two theories use very different estimates. For example, using their extrapolation, LES find the expected power in the dipole crustal field to be

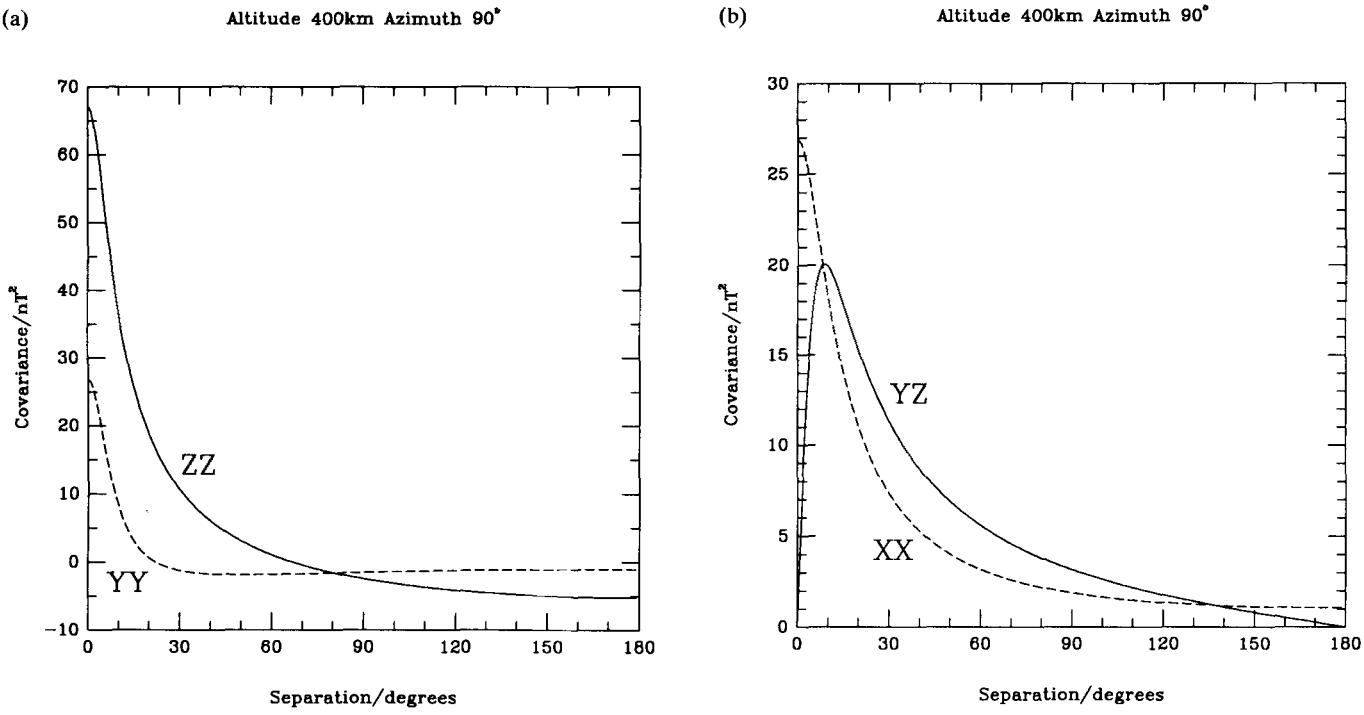

Figure 8. Correlation functions for different field components corresponding to Fig. 6 but using the theory of Langel *et al.* (1989). The altitude is 400 km, the azimuth is 90° and one point is on the equator. (a) Covariance of $\{ZZ\}$ and $\{YY\}$. (b) Covariance of $\{XY\}$ and $\{XX\}$.

$R_1 = 20\,\mathrm{nT}^2$. From equation (22), the theory presented here predicts $R_1 = 2 \times 10^{-3}\,\mathrm{nT}^2$ which is in considerable disagreement. The two theories at present represent rather extreme viewpoints; however, we believe that even when a more reasonable correlation length of a few tens of kilometres is used with this theory, the estimates of power at low degree will not change significantly.

To decide whether the theory presented here will be useful in improving models of the core field will require numerical calculations. However, some approximate comments can be made. To be of importance, we require that the eigenvectors and eigenvalues of $\mathbf{C}_e = \mathbf{C}_r + \mathbf{C}_c$ are somewhat different to those of $\mathbf{C}_r$, so that the linear combinations of data used in the fitting and the weights they are given are not the same as in the case where crustal correlations are ignored. The variance of crustal fields predicted by the theory presented here can be deduced from Fig. 7; the range in standard deviation is between 2.3 and 1.0 nT for X and Y and between 3.4 and 1.4 nT for Z over the altitude range 350–550 km. Now Langel *et al.* (1982) report the estimated root-sum-square value of errors due to instrument errors, position and time errors, digitization noise, attitude errors and spacecraft fields (but discounting external fields) to be 6 nT per Cartesian component for *Magsat*. The size of the residuals between data and typical field models is compatible with this figure (the misfit in Fig. 3 lies between 6.6 and 7.6 nT for example). For all except low-altitude *Magsat* data the size of the crustal signal is rather small in comparison, and it is unlikely that the use of $\mathbf{C}_e$ rather than $\mathbf{C}_r$ will alter field models enormously, although calculation is required to verify this. The effect will be more important in two circumstances: firstly if random errors are reduced [scalar data has an estimated random error of 2 nT (Langel *et al.* 1982), mainly because of the elimination of attitude errors]; and secondly, for the lowest altitude satellite data.

In this paper the crustal field has been dealt with using an idealized magnetic correlation function $\mathbf{M}$. The theory allows more realistic correlations to be used, but the observations are taken at a sufficiently large distance from the source region (the crust) that small changes in the magnetization correlation function $\mathbf{M}$ make only slight changes to $\mathbf{C}_c$. Objections could be made that the system has been oversimplified; for example, the statistics of crustal fields over continents may not be equivalent to those over oceans, which would negate our assumption of stationarity; our model is isotropic in direction, whereas seafloor spreading causes distinct directionality; and the depth to the Curie isotherm varies even over oceans with the age of the seafloor. Inclusion of all these effects requires a deterministic element in the model, and the stochastic model succeeds in reflecting the average physical effect to a large degree. The theory as it stands gives the prospect of improvement of models of the core magnetic field if it is applied to the calculation of an appropriate weight matrix $\mathbf{C}_e$ to be used in an inversion. Numerical aspects of this will be the subject of a future report.

ACKNOWLEDGMENTS

I am grateful to Jeremy Bloxham for many valuable discussions. I also thank David Gubbins, Jean-Louis LeMouël and Kathy Whaler for their help and interest. This work was begun whilst the author held a UK NERC Research Studentship at the Bullard Laboratories, University of Cambridge, and has subsequently been supported by NASA grant NAG5-918 and by NSF grant EAR88-04618.

REFERENCES

Abramowitz, M. & Stegun, I. A., eds, 1970. *Handbook of Mathematical Functions,* Dover, New York.

Arkani-Hamed, J. & Strangway, D. W., 1986. Band-limited global scalar magnetic anomaly map of the earth derived from magsat data, *J. geophys. Res.*, **91,** 8193–8203.

Backus, G. E., 1970. Inference from inadequate and inaccurate data, II, *Proc. Nat. Acad. Sci. USA,* **65,** 281–287.

Backus, G. E., 1975. Gross thermodynamics of heat engines in deep interior of earth, *Proc. Nat. Acad. Sci. USA,* **72,** 1555–1558.

Backus, G. E., 1983. Application of mantle filter theory to the magnetic jerk of 1969, *Geophys. J. R. astr. Soc.*, **74,** 713–746.

Backus, G. E., 1986. Poloidal and toroidal fields in geomagnetic field modelling, *Rev. Geophys.*, **24,** 75–109.

Backus, G. E., 1988a. Bayesian inference in geomagnetism, *Geophys. J.*, **92,** 125–142.

Backus, G. E., 1988b. Comparing hard and soft bounds in geophysical inverse problems, *Geophys. J.*, **94,** 249–261.

Backus, G. E., 1989. Confidence set inference with a prior quadratic bound, *Geophys. J.*, **97,** 119–150.

Benton, E. R. & Whaler, K. A., 1983. Rapid diffusion of a poloidal geomagnetic field through the weakly-conducting mantle: A perturbation solution, *Geophys. J. R. astr. Soc.*, **75,** 77–100.

Bloxham, J. & Jackson, A., 1989. Simultaneous stochastic inversion for geomagnetic main field and secular variation II: 1820–1980, *J. geophys. Res.*, **94,** 15 753–15 769.

Cain, J. C., Wang, Z., Kluth, C. & Schmitz, D. R., 1989. Derivation of a geomagnetic model to $n = 63$, *Geophys. J. Int.*, **97,** 431–441.

Constable, C. G. & Parker, R. L., 1988. Statistics of the geomagnetic secular variation for the past 5 m.y., *J. geophys. Res.*, **93,** 11 569–11 581.

Counil, J. L., Achache, J. & Cohen, Y., 1989. Global long wavelength magnetic signal induced by the ocean/continent susceptibility contrast, *IAGA Bull.*, **53,** 182.

Goff, J. A. & Jordan, T. H., 1988. Stochastic modeling of seafloor morphology: Inversion of sea beam data for second-order statistics, *J. geophys. Res.*, **93,** 13 589–13 608.

Gubbins, D., 1975. Can the earth's magnetic field be sustained by core oscillations?, *Geophys. Res. Lett.*, **2,** 409–412.

Gubbins, D., 1983. Geomagnetic field analysis—I. Stochastic inversion, *Geophys. J. R. astr. Soc.*, **73,** 641–652.

Gubbins, D. & Bloxham, J., 1985. Geomagnetic field analysis—III. Magnetic fields on the core–mantle boundary, *Geophys. J. R. astr. Soc.*, **80,** 695–713.

Hahn, A., Ahrendt, H., Meyer, J. & Hufen, J. H., 1984. A model of magnetic sources within the earth's crust compatible with the field measured by the satellite Magsat, *Geol. Jb. Hanover,* **75,** 125–156.

Hewitt, J. M., McKenzie, D. P. & Weiss, N. O., 1975. Dissipative heating in convective flows, *J. Fluid Mech.*, **68,** 721–738.

Jackson, J. D., 1975. *Classical Electrodynamics,* 2nd edn, John Wiley & Sons, New York.

LaBrecque, J. L. & Raymond, C. A., 1985. Seafloor spreading anomalies in the magsat field of the north atlantic, *J. geophys. Res.*, **90,** 2565–2575.

Langel, R. A. & Estes, R. H., 1982. A geomagnetic field spectrum, *Geophys. Res. Lett.*, **9,** 250–253.

Langel, R. A. & Estes, R. H., 1985. Large-scale, near-field

magnetic fields from external sources and the corresponding induced internal field, *J. geophys. Res.*, **90,** 2487–2494.

Langel, R. A., Estes, R. H. & Sabaka, T. J., 1989. Uncertainty estimates in geomagnetic field modelling, *J. geophys. Res.*, **94,** 12 281–12 299.

Langel, R., Ousley, G., Berbert, J., Murphy, J. & Settle, M., 1982. The magsat mission, *Geophys. Res. Lett.*, **9,** 243–245.

Lloyd, D. & Gubbins, D., 1990. Toroidal fluid motion at the top of the earth's core, *Geophys. J. Int.*, **100,** 455–467.

Lowes, F. J., 1966. Mean square values on sphere of spherical harmonic vector fields, *J. geophys. Res.*, **71,** 2179.

Lowes, F. J., 1974. Spatial power spectrum of the main geomagnetic field and extrapolation to the core, *Geophys. J. R. astr. Soc.*, **36,** 717–730.

Mauersberger, P., 1956. Das Mittel der Energiedichte des Geomagnetischen Hauptfeldes an der Erdoberfläche und seine säkulare Änderung, *Gerlands Beitr. Geophys.*, **65,** 207–215.

Mayhew, M. A., Johnson, B. D. & Wasilewski, P. J., 1985. A review of problems and progress in studies of satellite magnetic anomalies, *J. geophys. Res.*, **90,** 2511–2522.

Meyer, J., Hufen, J. H., Siebert, M. & Hahn, A., 1983. Investigations of the internal geomagnetic field by means of a global model of the earth's crust, *J. Geophys.*, **52,** 71–84.

Meyer, J., Hufen, J. H., Siebert, M. & Hahn, A., 1985. On the identification of magsat anomaly charts as crustal part of the internal field, *J. geophys. Res.*, **90,** 2537–2541.

Parker, R. L., 1971. The determination of seamount magnetism, *Geophys. J. R. astr. Soc.*, **24,** 321–324.

Parker, R. L., 1972. Inverse theory with grossly inadequate data, *Geophys. J. R. astr. Soc.*, **29,** 123–138.

Parker, R. L., 1988. A statistical theory of seamount magnetism, *J. geophys. Res.*, **93,** 3105–3115.

Parker, R. L. & Daniell, G. J., 1979. Interpretation of borehole magnetometer data, *J. geophys. Res.*, **84,** 5467–5479.

Parker, R. L. & Shure, L., 1982. Efficient modeling of the earth's magnetic field with harmonic splines, *Geophys. Res. Lett.*, **9,** 812–815.

Parker, R. L., Constable, C. & Stark, P. B., 1989. Recent core field models consistent with geophysical constraints, *IAGA Bull.*, **53,** 130.

Press, W. H., Flannery, B. P., Teukolsky, S. A. & Vetterling, W. T., 1986. *Numerical Recipes: the Art of Scientific Programming*, Cambridge University Press, Cambridge.

Ritzwoller, M. H. & Bentley, C. R., 1982. Magsat magnetic anomalies over antarctica and the surrounding oceans, *Geophys. Res. Lett.*, **9,** 285–288.

Roberts, P. H. & Scott, S., 1965. On analysis of the secular variation. 1. A hydromagnetic constraint: theory, *J. Geomagn. Geoelectr.*, **17,** 137–151.

Runcorn, S. K., 1975. On the interpretation of lunar magnetism, *Phys. Earth planet. Inter.*, **10,** 327–335.

Shure, L., Parker, R. L. & Backus, G. E., 1982. Harmonic splines for geomagnetic field modelling, *Phys. Earth planet. Inter.*, **28,** 215–229.

Shure, L., Parker, R. L. & Langel, R. A., 1985. A preliminary harmonic spline model from Magsat data, *J. geophys. Res.*, **90,** 11 505–11 512.

Tarantola, A., 1987. *Inverse Problem Theory. Methods for Data Fitting and Model Parameter Estimation*, Elsevier, Amsterdam.

Whaler, K. A. & Gubbins, D., 1981. Spherical harmonic analysis of the geomagnetic field: an example of a linear inverse problem, *Geophys. J. R. astr. Soc.*, **65,** 645–693.

APPENDIX A

This section discusses methods of calculating the induced magnetic field given an internal field model and a susceptibility distribution. In calculations we always use real Schmidt quasi-normalised spherical harmonics, but for notational convenience we refer to the set of harmonics of degree l as $\{Y_l^m\}$, $-l \le m \le l$, with a mapping of (for example)

$$P_l^m(\cos\theta)\cos m\phi \leftrightarrow Y_l^m(\theta,\phi) \quad ; \quad P_l^m(\cos\theta)\sin m\phi \leftrightarrow Y_l^{-m}(\theta,\phi) \quad ; \quad P_l^0(\cos\theta) \leftrightarrow Y_l^0(\theta,\phi) \tag{A1}$$

and

$$\oint Y_l^m Y_p^q \, d\Omega = \frac{4\pi}{2l+1}\delta_{lp}\delta_{mq}. \tag{A2}$$

We need to calculate the potential Φ given by

$$\Phi(\mathbf{r}_j) = -\mu_0^{-1}\int_V \chi \mathbf{H}_j(\mathbf{s})\cdot\nabla V_i \, d^3\mathbf{s} \tag{A3}$$

where V_i is the internal (inducing) field and $\mathbf{H}_j(\mathbf{s})$ is given by (7). If we take V to be only the continents $\mathcal{C}$ (defined by $C(\theta,\phi) = 1$ on $\mathcal{C}$ and $C(\theta,\phi) = 0$ otherwise), with upper boundaries at $r = a$ and $r = b = a - d$ and coastline $\partial\mathcal{C}$, and if χ is constant within V ($\chi = \chi_0$ say) then equation(A3) is expressible as a surface integral as

$$\Phi(\mathbf{r}_j) = -\chi_0\mu_0^{-1}\int_{\partial V} V_i \mathbf{H}_j(\mathbf{s})\cdot\hat{\mathbf{n}} \, d^3\mathbf{s} \tag{A4}$$

where ∂V is the surface of V. Now $\partial V = C(\theta,\phi)\,[\delta(r-a) + \delta(r-b)] + \partial C(\theta,\phi)\,[H(r-a) - H(r-b)]$ where $\delta(r)$ is the Dirac delta function and $H(r)$ the Heaviside function. The surfaces of V generate a potential of the form

$$\Phi(r,\theta,\phi) = a\sum_{l=1}^{\infty}\sum_{m=0}^{l}\left(\frac{a}{r}\right)^{l+1} Y_l^m(\theta,\phi)\tilde{\alpha}_l^m, \tag{A5}$$

where

$$\tilde{\alpha}_l^m = \alpha_l^m(a) - \left(\frac{b}{a}\right)^{l+1}\alpha_l^m(b) + \gamma_l^m. \tag{A6}$$

The γ_l^m are derived from the edge contribution, and the coefficients $\alpha_l^m(r)$ are generated by the top and bottom surfaces and are given by

$$\begin{aligned}\alpha_l^m(r) &= -\frac{\chi_0}{4\pi a} l \int_{\mathcal{C}} V(r,\theta,\phi) Y_l^m(\theta,\phi)\, d^2\hat{S} \\ &= -\frac{\chi_0}{4\pi a} l \int_{\Omega} C(\theta,\phi) V(r,\theta,\phi) Y_l^m(\theta,\phi)\, d\Omega. \end{aligned} \tag{A7}$$

If both $C(\theta,\phi)$ and $V(r,\theta,\phi)$ are descibed by spherical harmonic expansions, then (A7) is just an example of a *spherical transform* which can be performed accurately and efficiently using fast Fourier transforms and Gauss-Legendre quadrature (see e.g. Lloyd & Gubbins 1990). The edges of ∂V give a contribution represented by

$$\gamma_l^m \simeq -\frac{\chi_0 d}{4\pi a^2} \int_{\partial \mathcal{C}} V(a,\theta,\phi)\hat{\mathbf{n}} \cdot \nabla_{\mathrm{h}} Y_l^m(\theta,\phi)\, dl. \tag{A8}$$

The $\tilde{\alpha}_l^m$ can be mapped into the coefficients $\{i_l^m; j_l^m\}$ of the text by using a mapping similar to (A1).

Spherical Harmonic Representation of Continents

Let

$$C(\theta,\phi) = \begin{cases} 1 & \text{if} \quad (\theta,\phi) \in \mathcal{C} \\ 0 & \text{if} \quad (\theta,\phi) \notin \mathcal{C} \end{cases} \tag{A9}$$

where $\mathcal{C}$ represents the continents. Then the spherical harmonic representation of χ of the form

$$C(\theta,\phi) = \sum_{l=1}^{\infty} \sum_{m=-l}^{l} c_l^m Y_l^m(\theta,\phi) \tag{A10}$$

has coefficients given by

$$c_l^m = \frac{2l+1}{4\pi} \int_{\mathcal{C}} Y_l^m(\theta,\phi)\, d\Omega. \tag{A11}$$

Now following Shure *et al.* (1985) and using the fact that on the unit sphere $\nabla_{\mathrm{h}}^2 Y_l^m = -l(l+1)Y_l^m$, equation (A11) can be written as a line integral along $\partial\mathcal{C}$, the boundary of $\mathcal{C}$, as

$$c_l^m = -\frac{2l+1}{4\pi l(l+1)} \int_{\partial \mathcal{C}} \hat{\mathbf{n}} \cdot \nabla_{\mathrm{h}} Y_l^m(\theta,\phi)\, dl. \tag{A12}$$

For the calculations reported in the text, the integral was performed by quadrature with an average distance between points on the boundary of 0.6°.

APPENDIX B

The magnetic field due to the crust $\Delta\mathbf{B}$ measured by satellite is related to the magnetostatic potential ϕ_m by $\Delta\mathbf{B} = -\nabla\phi_m$, where

$$\phi_m(\mathbf{r}_j) = \int_V \mathbf{H}_j(\mathbf{s}) \cdot \mathbf{M}(\mathbf{s})\, d^3\mathbf{s} \tag{B1}$$

and $\mathbf{H}_j(\mathbf{s})$ (the Green's function for the potential) is given in (7).

In what follows we use greek superscripts to indicate the component of field, and roman subscripts to indicate the position of observation. Then, for example, $\Delta B_j^{(\eta)}$ represents the η component of field $\Delta\mathbf{B}$ at position $\mathbf{r}_j$.

In a spherical coordinate system where θ is colatitude, ϕ is longitude and $r = |\mathbf{r}|$ is radius, each cartesian component of $\Delta\mathbf{B} = (\Delta X, \Delta Y, \Delta Z)$ in the $(-\hat{\boldsymbol{\theta}}, \hat{\boldsymbol{\phi}}, -\hat{\mathbf{r}})$ directions is related to the magnetization $\mathbf{M}$ of the crust by

$$\Delta B^{(\eta)}(\mathbf{r}_j) = -\hat{\boldsymbol{l}}_j^{(\eta)} \cdot \nabla_{\mathbf{r}_j} \int_V \mathbf{H}_j(\mathbf{s}) \cdot \mathbf{M}(\mathbf{s})\, d^3\mathbf{s}, \tag{B2}$$

where $\nabla_{\mathbf{r}_j}$ means differentiation with respect to $\mathbf{r}_j$, and $\hat{\boldsymbol{l}}_j^{(\eta)}$ is defined in (B3) below. For measurements of cartesian components X, Y, and Z, linearity implies that the errors in measurements due to the crust $e_i^{(\eta)}$ are equal to the crustal field components themselves: $e_i^{(\eta)} = \Delta B_i^{(\eta)}$ for $\eta = X, Y, Z$. Errors in measurements of scalar intensity $F = |\mathbf{B}|$ can be treated, since the crustal perturbation $\Delta\mathbf{B}$ is very much smaller than the main geomagnetic field $\mathbf{B}_0$. Therefore errors are well represented by $e_i^{(F)} \simeq \hat{\mathbf{B}}_0(\mathbf{r}_i) \cdot \Delta\mathbf{B}(\mathbf{r}_i)$, where $\hat{\mathbf{B}}_0(\mathbf{r}_i)$ is a unit vector in the direction of the main geomagnetic field at position $\mathbf{r}_i$. Therefore errors in F are linear in the magnetization $\mathbf{M}$, but they do assume knowledge of the main field

$\mathbf{B}_0$. Since these functions are used only for error estimation, a preliminary internal field model is probably adequate for this purpose. The Green's functions relating all four types of crustal field errors $e_i^{(\eta)}$ of interest to the magnetization $\mathbf{M}$ can be written

$$\mathbf{G}^{(\eta)}(\mathbf{r}_j,\mathbf{s}) = -\hat{\boldsymbol{l}}_j^{(\eta)} \cdot \nabla_{\mathbf{r}_j}\mathbf{H}(\mathbf{r}_j,\mathbf{s}) \quad \text{where} \quad \hat{\boldsymbol{l}}_j^{(\eta)} = \begin{cases} -\hat{\boldsymbol{\theta}} & \eta = X \\ \hat{\boldsymbol{\phi}} & \eta = Y \\ -\hat{\mathbf{r}} & \eta = Z \\ \hat{\mathbf{B}}_0(\mathbf{r}_j) & \eta = F \end{cases} \tag{B3}$$

Following Parker (1971) the Gram matrix Γ can be written as

$$\Gamma_{ij}^{(\eta\nu)} = \left(\frac{\mu_0}{4\pi}\right)^2 \hat{\boldsymbol{l}}_i^{(\eta)} \cdot \nabla_{\mathbf{r}_i}\hat{\boldsymbol{l}}_j^{(\nu)} \cdot \nabla_{\mathbf{r}_j}\Upsilon(\mathbf{r}_i,\mathbf{r}_j) \tag{B4}$$

where

$$\Upsilon(\mathbf{r}_i,\mathbf{r}_j) = \int_V \nabla F_i \cdot \nabla F_j \, d^3\mathbf{s} \quad \text{with} \quad F_j = \frac{1}{|\mathbf{r}_j - \mathbf{s}|}. \tag{B5}$$

Adopting the magnetization correlation tensor (16) , we see that Υ measures the correlation between potential since

$$E\{\phi_m(\mathbf{r}_j)\phi_m(\mathbf{r}_k)\} = \beta^2 \left(\frac{\mu_0}{4\pi}\right)^2 \Upsilon(\mathbf{r}_j,\mathbf{r}_k). \tag{B6}$$

Υ can be written as a surface integral since

$$\nabla F_j \cdot \nabla F_k = \nabla \cdot (F_j \nabla F_k) - F_j \nabla^2 F_k \tag{B7}$$

and all the measurement positions $\mathbf{r}_k$ lie outside the magnetized volume (the crust), so $\nabla^2|\mathbf{r}_k - \mathbf{s}|^{-1} = 0$ and the last term on the right-hand side is zero. Then using Gauss's theorem,

$$\Upsilon(\mathbf{r}_i,\mathbf{r}_j) = \int_{\partial V} F_i \nabla F_j \cdot \hat{\mathbf{n}}(\mathbf{s}) \, d^2\mathbf{s} \tag{B8}$$

where $\hat{\mathbf{n}}(\mathbf{s})$ is the unit normal to the surface at $\mathbf{s}$. For the crustal model, ∂V consists of two concentric spheres at the top and bottom of the crust. Thus evaluating Υ involves performing two integrals of the form

$$I(\mathbf{r}_j,\mathbf{r}_k,s) = \int_{|\mathbf{s}|=s} \frac{1}{|\mathbf{r}_j - \mathbf{s}|} \frac{\partial}{\partial r}\left\{\frac{1}{|\mathbf{r}_k - \mathbf{s}|}\right\} d^2\mathbf{s} \tag{B9}$$

over the spheres of radii $s_1 = a$ and $s_2 = b = a - d$ where a is the radius of the Earth and d is the depth of the magnetic layer. To proceed, recall that the generating function for Legendre polynomials can be written as

$$\frac{1}{|\mathbf{r}_k - \mathbf{s}|} = \frac{1}{s}\sum_{n=0}^{\infty}\left(\frac{s}{r_k}\right)^{n+1} P_n(\mu_k) \tag{B10}$$

where μ_k is the cosine of the angle between $\mathbf{r}_k$ and $\mathbf{s}$, and substitute into equation (B9). To perform the integral we need to apply the addition theorem for complex fully-normalised spherical harmonics (e.g. Jackson 1975):

$$P_l(\mu_k) = \frac{4\pi}{2l+1}\sum_{m=-l}^{l} Y_l^m(\theta,\phi)Y_l^{m*}(\theta_k,\phi_k). \tag{B11}$$

Then (B9) becomes

$$\begin{aligned} I(\mathbf{r}_j,\mathbf{r}_k,s) &= \int_{|\mathbf{r}|=s} \frac{1}{r}\sum_{n=0}^{\infty}\left(\frac{r}{r_j}\right)^{n+1} P_n(\mu_j)\frac{\partial}{\partial r}\left\{\frac{1}{r}\sum_{l=0}^{\infty}\left(\frac{r}{r_k}\right)^{l+1} P_l(\mu_k)\right\} r^2 d\Omega \\ &= \int_{|\mathbf{r}|=s} \frac{1}{r}\sum_{n=0}^{\infty}\sum_{p=-n}^{n}\frac{4\pi}{2n+1}\left(\frac{r}{r_j}\right)^{n+1} Y_n^p(\theta,\phi)Y_n^{p*}(\theta_j,\phi_j) \\ &\quad \times \frac{1}{r_k^2}\sum_{l=0}^{\infty}\sum_{m=-l}^{l}\frac{4\pi}{2l+1} l\left(\frac{r}{r_k}\right)^{l-1} Y_l^{m*}(\theta,\phi)Y_l^m(\theta_k,\phi_k) r^2 \, d\Omega \end{aligned} \tag{B12}$$

where Ω is solid angle. Using the orthogonality of the spherical harmonics and a re-application of the addition theorem leads to the result that $I(\mathbf{r}_j,\mathbf{r}_k,s)$ can be written in the form

$$I(\mathbf{r}_j,\mathbf{r}_k,s) = \frac{4\pi}{s} Q(\mu_{jk},\rho) \tag{B13}$$

with

$$Q(\mu,\rho)=\sum_{l=0}^{\infty}\frac{l}{2l+1}\rho^{l+1}P_l(\mu)\quad\text{where}\quad\rho=\left(\frac{s^2}{r_jr_k}\right)\tag{B14}$$

and μ_{jk} is the cosine of the angle between the vectors $\mathbf{r}_j$ and $\mathbf{r}_k$. Collecting together all the terms, the final form for the covariance tensor is

$$[\mathsf{C}_c]_{ij}^{(\eta\nu)}=E\{e_i^{(\eta)}e_j^{(\nu)}\}=\beta^2\left(\frac{\mu_0}{4\pi}\right)^2\hat{\boldsymbol{l}}_i^{(\eta)}\cdot\nabla_{\mathbf{r}_i}\hat{\boldsymbol{l}}_j^{(\nu)}\cdot\nabla_{\mathbf{r}_j}\left[I(\mathbf{r}_i,\mathbf{r}_j,a)-I(\mathbf{r}_i,\mathbf{r}_j,b)\right]\tag{B15}$$

with I given above.

Similar forms for matrix elements can be found in Shure *et al.* (1982), although in their application, by a judicious choice of quelling (Backus 1970), it was possible to rewrite the infinite sums for the Gram matrix elements similar to (B14) which appeared in their work in terms of closed-form analytic functions. Here the Gram matrix elements are dictated by the statistical theory, and no such quelling is possible.

It is desirable for numerical speed and accuracy that the infinite sums for Q, or at least its derivatives, be put into closed form. Unfortunately, the sums lead to rather cumbersome functions. We show how the sums which are required for this theory are performed; the same methods can be applied to other infinite sums such as the ones given in Langel *et al.* (1989). Consider first the generating function:

$$\frac{1}{\sqrt{1-2\mu\rho+\rho^2}}=\sum_{l=0}^{\infty}\rho^lP_l(\mu).\tag{B16}$$

Multiplying both sides by $\rho^{-1/2}$ and integrating leads to the result

$$\int_0^{\rho}\frac{1}{\sqrt{\rho'(1-2\mu\rho'+\rho'^2)}}\,d\rho'=2\sqrt{\rho}\sum_{l=0}^{\infty}\frac{\rho^l}{2l+1}P_l(\mu).\tag{B17}$$

The integral on the left-hand-side can be evaluated numerically by quadrature, but it is more instructive to note that it is an elliptic integral of the first kind, written as

$$F(\phi,k)=\int_0^{\phi}\frac{1}{\sqrt{1-k^2\sin^2\phi'}}\,d\phi'\tag{B18}$$

with arguments

$$\begin{aligned}\phi(\rho)&=2\arctan\sqrt{\rho}\\ k(\mu)&=\sqrt{(1+\mu)/2}.\end{aligned}$$

With this identification, sums such as (B14) can easily be performed. For measurements at the earth's surface, $\rho=1$ and $\phi=\pi/2$, and $F(\phi,k)$ becomes a complete elliptic integral of the first kind, $K(k)$ (see Abramowitz & Stegun 1970), which is divergent as $\mu\to 0$, a consequence of the magnetization tensor M chosen (see (16)). Table 1 lists the derivatives of Q with respect to μ and ρ in terms of F and E (elliptic integrals of the first and second kinds) and closed form functions.

The infinite sums have been used to check the accuracy of the elements given in Table 1, since for satellite measurements $\rho<1$ in equation (B14) and therefore all the series for Q and its derivatives, found from term-by-term differentiation, are unconditionally convergent, and can be truncated when the terms reach machine precision. For example, when $\mu_{ij}=1$, the most slowly-converging series corresponding to the expressions in Table 1 is $\partial^2Q/\partial\mu^2$, because $P_l''(1)=(l-1)l(l+1)(l+2)/8$ and so terms in the series form (B14) for $\partial^2Q/\partial\mu^2$ are $\mathcal{O}(l^4\rho^l)$. Consequently, when $\mathbf{r}_i=\mathbf{r}_j=400\,\text{km}$, the series form for $\partial^2Q/\partial\mu^2$ requires approximately 350 terms to reach single-precision accuracy.

The subroutine *el2* of Press *et al.* (1986) has been used to evaluate the elliptic integrals of both the first and second kinds, $F(\phi,k)$ and $E(\phi,k)$ respectively (see Table 1).

Evaluation of Matrix Elements

To evaluate the matrix elements we require the derivatives appearing in equation (B15). If $\partial/\partial\alpha_i$ represents either $\partial/\partial r_i$, $(1/r_i)\,\partial/\partial\theta_i$, $-(1/r_i\sin\theta_i)\,\partial/\partial\phi_i$ (appropriate for X, Y, Z data), then

$$\frac{\partial^2Q}{\partial\alpha_i\partial\alpha_j}=\frac{\partial^2\mu}{\partial\alpha_i\partial\alpha_j}\frac{\partial Q}{\partial\mu}+\frac{\partial^2\rho}{\partial\alpha_i\partial\alpha_j}\frac{\partial Q}{\partial\rho}+\frac{\partial\rho}{\partial\alpha_i}\frac{\partial\rho}{\partial\alpha_j}\frac{\partial^2Q}{\partial\rho^2}+\frac{\partial\mu}{\partial\alpha_i}\frac{\partial\mu}{\partial\alpha_j}\frac{\partial^2Q}{\partial\mu^2}+\left(\frac{\partial\rho}{\partial\alpha_i}\frac{\partial\mu}{\partial\alpha_j}+\frac{\partial\mu}{\partial\alpha_i}\frac{\partial\rho}{\partial\alpha_j}\right)\frac{\partial^2Q}{\partial\rho\partial\mu}.\tag{B19}$$

The necessary derivatives of Q are listed in Table 1, and for completeness the forms for ρ, the reciprocal reduced radius, and μ_{ij}, the cosine of the angular separation of $\mathbf{r}_i$ and $\mathbf{r}_j$, and their appropriate derivatives are listed in Table 2. Some of the derivatives of Q require special attention in the limit $\mu=1$, so these forms are listed separately in Table 3.

Then the matrix elements are, for example,

$$E\left\{\epsilon^{(Y)}(\mathbf{r}_i)e^{(Y)}(\mathbf{r}_j)\right\} = k(\beta)\rho_1\left\{\frac{\partial^2\Delta Q}{\partial\mu^2}\frac{1}{\sin\theta_i}\frac{\partial\mu_{ij}}{\partial\phi_i}\frac{1}{\sin\theta_j}\frac{\partial\mu_{ij}}{\partial\phi_j}+\frac{\partial\Delta Q}{\partial\mu}\frac{1}{\sin\theta_i\sin\theta_j}\frac{\partial^2\mu_{ij}}{\partial\phi_i\partial\phi_j}\right\} \tag{B20}$$

where

$$\Delta Q = Q(\mu,\rho_1) - (s_1/s_2)\,Q(\mu,\rho_2) \tag{B21}$$

and s_1 and s_2 are the outer and inner radii of the shell given below (B9), ρ_1 and ρ_2 are given by (B14) for $s_1 = a$ and $s_2 = b$, and $k(\beta) = \beta^2\mu_0^2/4\pi a^3$.

Table 1. Derivatives of Q required to compute the matrix elements. For the case $\mu = 1$ see Table 3.

$$\begin{aligned}
Q &= \frac{\rho}{2R} - \frac{\sqrt{\rho}F}{4}\\
\frac{\partial Q}{\partial\rho} &= \frac{1}{4R} - \frac{F}{8\sqrt{\rho}} - \frac{\rho(\rho-\mu)}{2R^3}\\
\frac{\partial^2 Q}{\partial\rho^2} &= \frac{F}{16\rho^{\frac{3}{2}}} - \frac{1}{8R\rho} + \frac{3\rho(\rho-\mu)^2}{2R^5} - \frac{5\rho-3\mu}{4R^3}\\
\frac{\partial Q}{\partial\mu} &= \frac{F\sqrt{\rho}}{16k^2} - \frac{E\sqrt{\rho}}{16k^2{k_c}^2} + \frac{\rho^2}{2R^3} + \frac{\sqrt{\rho}\cos\phi\sin\phi}{16\Delta{k_c}^2}\\
\frac{\partial^2 Q}{\partial\mu\partial\rho} &= \frac{F}{32k^2\sqrt{\rho}} - \frac{E}{32k^2{k_c}^2\sqrt{\rho}} + \frac{\rho}{R^3} - \frac{3\rho^2(\rho-\mu)}{2R^5} + \frac{\cos\phi\sin\phi}{32\Delta{k_c}^2\sqrt{\rho}} - \frac{\sin^2\phi}{16\Delta^3(1+\rho)}\\
\frac{\partial^2 Q}{\partial\mu^2} &= \frac{E\left(1-2k^2\right)\sqrt{\rho}}{32k^4{k_c}^4} + \frac{F\left(1-3{k_c}^2\right)\sqrt{\rho}}{64k^4{k_c}^2} + \frac{3\rho^3}{2R^5} + \frac{\sqrt{\rho}\cos\phi\sin\phi\left[\Delta^2\left(3k^2-1\right)+k^2{k_c}^2\sin^2\phi\right]}{64\Delta^3k^2{k_c}^4}
\end{aligned}$$

where

$$\begin{aligned}
\phi(\rho) &= 2\arctan\sqrt{\rho} && \text{Amplitude}\\
k(\mu) &= \sqrt{(1+\mu)/2} && \text{Modulus}\\
k_c(\mu) &= \sqrt{1-k^2} && \text{Complementary modulus}\\
\Delta(\phi,k) &= \sqrt{1-k^2\sin^2\phi} && \text{Delta amplitude}\\
F(\phi,k) &= \int_0^\phi \Delta(\phi',k)^{-1}\,d\phi'\\
&= \int_0^\phi 1/\sqrt{1-k^2\sin^2\phi'}\,d\phi' && \text{Elliptic Integral of First Kind}\\
E(\phi,k) &= \int_0^\phi \Delta(\phi',k)\,d\phi'\\
&= \int_0^\phi \sqrt{1-k^2\sin^2\phi'}\,d\phi' && \text{Elliptic Integral of Second Kind}\\
R(\mu,\rho) &= \sqrt{1-2\mu\rho+\rho^2}
\end{aligned}$$

Table 2. Derivatives of μ and ρ required to compute the matrix elements.

$$
\begin{aligned}
\rho &= \frac{s^2}{r_i r_j} \\
\frac{\partial \rho}{\partial r_i} &= -\frac{\rho}{r_i} \\
\frac{\partial^2 \rho}{\partial r_i \partial r_j} &= \frac{\rho}{r_i r_j} \\
\mu_{ij} &= \cos\theta_i \cos\theta_j + \cos(\phi_i - \phi_j) \sin\theta_i \sin\theta_j \\
\frac{\partial \mu_{ij}}{\partial \theta_i} &= -\sin\theta_i \cos\theta_j + \cos\theta_i \sin\theta_j \cos(\phi_i - \phi_j) \\
\frac{\partial \mu_{ij}}{\partial \theta_j} &= -\cos\theta_i \sin\theta_j + \sin\theta_i \cos\theta_j \cos(\phi_i - \phi_j) \\
\frac{\partial^2 \mu_{ij}}{\partial \theta_i \partial \theta_j} &= \sin\theta_i \sin\theta_j + \cos\theta_i \cos\theta_j \cos(\phi_i - \phi_j) \\
\frac{1}{\sin\theta_i} \frac{\partial \mu_{ij}}{\partial \phi_i} &= -\sin\theta_j \sin(\phi_i - \phi_j) \\
\frac{1}{\sin\theta_j} \frac{\partial \mu_{ij}}{\partial \phi_j} &= \sin\theta_i \sin(\phi_i - \phi_j) \\
\frac{1}{\sin\theta_i} \frac{\partial^2 \mu_{ij}}{\partial \phi_i \partial \theta_j} &= -\cos\theta_j \sin(\phi_i - \phi_j) \\
\frac{1}{\sin\theta_j} \frac{\partial^2 \mu_{ij}}{\partial \theta_i \partial \phi_j} &= \cos\theta_i \sin(\phi_i - \phi_j) \\
\frac{1}{\sin\theta_i \sin\theta_j} \frac{\partial^2 \mu_{ij}}{\partial \phi_i \partial \phi_j} &= \cos(\phi_i - \phi_j)
\end{aligned}
$$

Table 3. Derivatives of Q required to compute the matrix elements for the special case $\mu = 1$.

$$
\begin{aligned}
Q|_{\mu=1} &= \frac{\rho}{2(1-\rho)} - \frac{L\sqrt{\rho}}{4} \\
\left.\frac{\partial Q}{\partial \rho}\right|_{\mu=1} &= \frac{1+\rho}{4(1-\rho)^2} - \frac{L}{8\sqrt{\rho}} \\
\left.\frac{\partial^2 Q}{\partial \rho^2}\right|_{\mu=1} &= \frac{1+\rho}{2(1-\rho)^3} + \frac{1}{4(1-\rho)^2} - \frac{1}{8(1-\rho)\rho} + \frac{L}{16\rho^{\frac{3}{2}}} \\
\left.\frac{\partial Q}{\partial \mu}\right|_{\mu=1} &= \frac{\rho^2}{2(1-\rho)^3} - \frac{\rho}{8(1-\rho)^2} + \frac{\rho}{16(1-\rho)} + \frac{L\sqrt{\rho}}{32} \\
\left.\frac{\partial^2 Q}{\partial \mu \partial \rho}\right|_{\mu=1} &= \frac{3\rho^2}{2(1-\rho)^4} + \frac{3\rho}{4(1-\rho)^3} - \frac{2-\rho}{16(1-\rho)^2} + \frac{3}{32(1-\rho)} + \frac{L}{64\sqrt{\rho}} \\
\left.\frac{\partial^2 Q}{\partial \mu^2}\right|_{\mu=1} &= \frac{3\rho^3}{2(1-\rho)^5} - \frac{3\rho}{16(1-\rho)^4} + \frac{9\rho}{32(1-\rho)^3} - \frac{3\rho}{128(1-\rho)^2} - \frac{9\rho}{256(1-\rho)} - \frac{9L\sqrt{\rho}}{512}
\end{aligned}
$$

where

$$L = \log\left[\frac{1+\sqrt{\rho}}{1-\sqrt{\rho}}\right]$$